Korean J. Chem. Eng., 38(7), 1394-1402 (2021)
DOI: 10.1007/s11814-021-0823-3

pISSN: 0256-1115
eISSN: 1975-7220

Preparation and characteristics of wavy form microchannel reactors coated with H-ZSM-5 for the endothermic decomposition reaction of methylcyclohexane

Byeong Jun Jeong*, Min Chang Shin*, Byung Hun Jeong, and Jung Hoon Park*,†**

*Department of Biochemical and Chemical Engineering, Dongguk University, Seoul 04620, Korea
**Agency for Defense Development, Jochiwongil 462, Daejeon, Yuseong 34186, Korea
(*Received 2 January 2021 • Revised 25 March 2021 • Accepted 26 April 2021*)

Abstract−Endothermic decomposition reaction of methylcyclohexane (MCH) was conducted to solve problems of hypersonic flight as cooling technology. A wavy form microchannel reactor (WMCR) coated with H-ZSM-5 was used to improve this reaction. WMCR coated with H-ZSM-5 was simply prepared by using binder coating method. Field emission scanning electron microscope (FE-SEM) and energy dispersive spectroscopy (EDS) analysis were used to examine the surface of WMCR coated with H-ZSM-5. Endothermic decomposition reaction of MCH was carried out in a flow reactor under supercritical conditions (823 K and 50 bar) during 30 min. The liquid products produced by catalytic reaction were analyzed by gas chromatograph-mass selective detector (GC-MSD) at 10, 20 and 30 min, respectively. The results show that an increase in H-ZSM-5 coating amount on WMCR surface for catalytic reaction had a trade-off relationship; the increase of catalysts on WMCR had a positive effect on overall improvement of heat sink (from 416.59 kJ/mol to 611.06 kJ/mol) but simultaneously negative effect for catalytic life time because of increase in catalytic deactivation (from 5.9% to 30%).

Keywords: Wavy Form Microchannel Reactor, H-ZSM-5, Binder Coating, Heat Sink, Catalytic Deactivation

INTRODUCTION

Hypersonic flight vehicles are defined as flights that perform over Mach 5. Over Mach 7, the surface temperature of a flight vehicle and engine is higher than 2,273 K due to air friction. Because of this phenomenon, serious problems such as overheating of the engine, blocking of a combustion inlet, and degradation of flight durability can occur during flight. To solve these problems, the use of insulation and other coolants is not suitable because of increase in flight vehicle weight. Therefore, development of cooling technology to decrease temperature of the flight vehicle surface and engine is necessary to solve these problems [1-8].

Recently, to solve these problems various studies used endothermic fuels as cooling technology [9-15]. If hydrocarbon fuels of complex type are used as endothermic fuels, accurate analysis of their characteristics is difficult. Therefore, hydrocarbon fuels of simple type like methylcyclohexane (MCH) [16-18], n-dodecane [19-21], decalin are suitable as endothermic model fuels. Song and co-workers selected n-dodecane as endothermic fuel and compared the catalytic reaction of ZSM-5 and air-oxidized activated charcoal under supercritical conditions [20]. In addition, Liu et al. reported cooling technology by using n-dodecane as fuel and stainless steel tube coated with H-ZSM-5 [21]. Because MCH is a simple type of hydrocarbon fuel, such as n-dodecane, and has economical advantage, MCH was adopted as endothermic fuel in this study.

For improvement of endothermic decomposition reaction of hydrocarbon fuel, the choice of catalyst should be significantly considered. Because a combustor of hypersonic flight vehicles is in supercritical conditions, thermal stability of catalyst must be considered. Zeolite as catalyst with weak acid site and strong acid site is appropriate for improvement of the catalytic reaction [22,23]. Because zeolites of ZSM-5 type have high ratio of SiO_2/Al_2O_3 and micro pores of about 5 Å size, these catalysts not only have excellent thermal stability but also catalytic activation [24-26]. Therefore, zeolite of ZSM-5 type was used for improvement of catalytic reaction of hydrocarbon fuel in this study.

Catalysts of pellet type have some problems, such as the pressure drop, degradation of thermal stability and difficulty of pore structure control. However, if a coating method on substrate surface is used for catalytic reaction, the mentioned problems can be solved. In addition, using the coating method has some advantages, such as coke inhibition and improvement of catalytic activity [27-31]. Yang et al. used a coating method using hydrothermal synthesis for preparation of NaA nano-zeolite film on porous stainless steel microchannel [32]. Truter et al. used a coating method using Si binder for preparation of steel microreactor plates coated with the H-ZSM-5 zeolite [33]. A coating method using binder has some advantages, like simple and short coating process as compared to coating method using hydrothermal synthesis. Based on these reasons, the binder coating method was selected for preparation of wavy form microchannel reactors coated with H-ZSM-5 in this study.

Compared to general tube reactors, microchannel reactors have some advantages such as high surface-volume ratio, improvement of heat and mass transfer from decrease in diffusional path. For these reasons, microchannel reactors are potential implements for

†To whom correspondence should be addressed.
E-mail: pjhoon@dongguk.edu
Copyright by The Korean Institute of Chemical Engineers.

catalytic reaction [34-38]. In this study, a microchannel reactor with wavy form was adopted for catalytic reaction because surface-volume ratio of a wavy form microchannel reactor is high compared to linear form microchannel reactor with the same number of channels.

The purpose of this study is to confirm characteristics of wavy form microchannel reactors coated with different amount of H-ZSM-5 respectively. Finally, we confirmed the relationship between catalytic activity and coating amount of H-ZSM-5, and verified that the wavy form microchannel can apply to the endothermic reactor through certifying the effect of reactor geometry on catalytic performance.

EXPERIMENTAL

1. Materials

Methylcyclohexane (MCH, Junsei chemical Co., 99.0%) was used as hydrocarbon fuel for endothermic decomposition reaction. To prepare H-ZSM-5 with catalytic activation, NH_4-ZSM-5 (CBV-2314, Zeolyst Co., SiO_2/Al_2O_3=23) was calcined at 823 K for 4 h [5]. Wavy form microchannel reactor (WMCR) was prepared by vending stainless steel plate (stainless steel 316L, Innowill Co., 50 mm×120 mm×0.1 mm). The number of channels was nine, and widths of channels were 2.59 mm and 1.32 mm respectively. Tetraethylorthosilicate (TEOS, Sigma Aldrich, 98.0%) was used as Si binder for binder coating. Distilled water and nitric acid (Samchun Pure Chem Co., 60.0%) were used for hydrolysis of TEOS, and ethanol (Samchun Pure Chem Co., 99.9%) was used as solvent for preparation of binder coating sol.

2. Pretreatment of WMCR

Prior to binder coating process, WMCR was pretreated for enhancement of adhesion between microchannel surface and H-ZSM-5. First, WMCR was immersed in 0.1 M potassium hydroxide solution for removal of impurities at ultrasonic bath for 10 min. Thereafter, this reactor was immersed in 0.1 M nitric acid solution to increase roughness of surface at 353 K for 10 min, and then this reactor was immersed in distilled water and acetone at ultrasonic bath for washing surface for 10 min, respectively. Finally, to form an oxide layer on the surface, the treated reactor was calcined in a muffle furnace with 1,073 K for 4 h at air atmosphere.

3. Preparation of WMCR Coated with H-ZSM-5

Two-step processes were required for binder coating. First step was hydrolysis of TEOS for preparation of Si binder. 1 M TEOS, 100 M H_2O and 0.5 M HNO_3 were mixed by stirring with 150 rpm for 5 h at room temperature (298 K) [39]. Second step was preparation of coating sol for binder coating. H-ZSM-5 (20 wt%), Si binder (20 wt%) and ethanol (60 wt%) were mixed by stirring 150 rpm for 1 h at room temperature (298 K). Thereafter, pretreated WMCR was immersed in coating sol for 30 min, and then excess coating sol on surface was removed by blowing N_2 (99.999%, Seoul Special Gas Co.). The treated reactor was dried at room temperature (298 K) for 5 min, and was dried in oven at 423 K for 1 h. The dried reactor was thoroughly rinsed by using distilled water and then dried in oven at 343 K for 1 h. Finally, WMCR coated with H-ZSM-5 was calcined in the muffle furnace at 823 K for 4 h. The prepared reactors were labeled n-binder coated WMCR, where n means the number of binder coating cycles.

4. Characteristic of WMCR Coated with H-ZSM-5

Field emission scanning electron microscopy (FE-SEM, mod.S-4800, Hitachi, Japan) analysis and energy dispersive spectroscopy (EDS, mod.S-4800, Hitachi, Japan) analysis were conducted to examine the pretreated and H-ZSM-5 coated WMCR surface, and confirm thickness of H-ZSM-5 layer on WMCR. Cumulative H-ZSM-5 loading percent (wt%) was recorded about n-binder coated

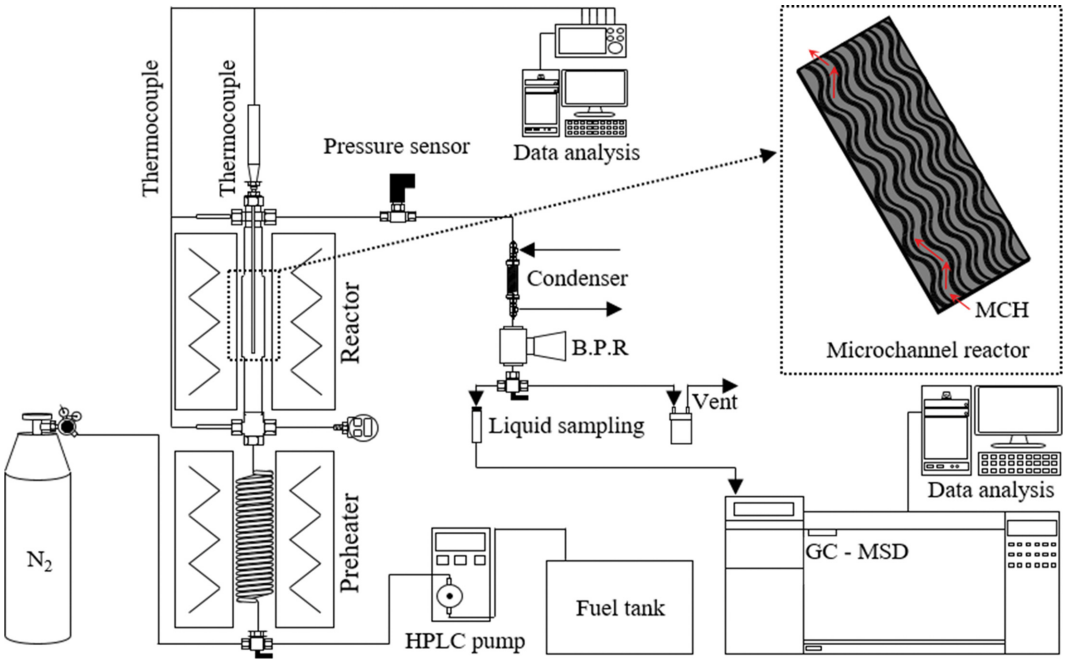


Fig. 1. Schematic diagram of microchannel reactor for an endothermic decomposition reaction of MCH.

WMCR (n=1, 2, 3, 4, 5), respectively, and an ultrasonic test was performed to test binding force between surface of reactor and H-ZSM-5 about each sample [40].

5. Catalytic Reaction

A schematic diagram of flow reactor using wavy form microchannel is presented in Fig. 1. Before catalytic reaction, N_2 (99.999%, Seoul Special Gas Co.) was blown in the reactor to remove oxygen and other impurities existing in the reactor. Thereafter, a pressure of reactor was set at 50 bar by using back pressure regulator (B. P. R.) and temperature of preheater and reactor was set at 673 K and 823 K, respectively. MCH at room temperature was supplied to preheater by using HPLC pump at 3 ml/min. During the catalytic reaction, to determine MCH conversion and composition of liquid products, liquid product sampling was conducted at 10, 20, 30 min, respectively. Analysis of liquid products was performed by using gas chromatograph-mass selective detector (GC-MSD, Agilent 6890 Gas Chromatograph-Agilent 5973 Mass selective detector) and HP-5 ms column.

6. Coke Analysis

After catalytic reaction, coke analysis about all WMCRs was conducted. Coke analysis was generally performed by using thermogravimetric analysis (TGA) [6] or temperature programmed oxidation (TPO) [19]. However, in this study, TGA and TPO analysis was not adopted to analyze coke because of morphology of WMCR. Therefore, coke analysis was conducted by using other method with conditions similar to TGA or TPO analysis in this study. First, to remove impurities except for coke on WMCR surface, air (99.999%, Dong-A Special Gas Co.) was blown in WMCR for 10 min at 0.5 ml/min. Thereafter, temperature of WMCR was set 923 K with air blowing at the same flow rate for 3 h. Finally, weight loss about all WMCRs was calculated by comparing weight of WMCR before coke analysis and weight of WMCR after coke analysis.

RESULTS AND DISCUSSION

1. Characteristic of Pretreated WMCR

To compare WMCR surface with and without pretreatment process, SEM image and EDS analysis were performed. Fig. 2(a) and (b) show SEM image of non-pretreated WMCR surface and pretreated WMCR surface, respectively. Depending on pretreatment process, roughness and porosity of WMCR surface were higher than non-pretreated WMCR. Table 1(a) and (b) show EDS data for non-pretreated WMCR surface and pretreated WMCR. Weight percentage of oxygen increased from 2.20% to 23.51% according to the pretreatment process. As results of SEM image and EDS analysis, porous oxide layer was formed on WMCR surface through the pretreatment process.

Table 1. EDS data for the microchannel (a) before pretreatment, (b) after pretreatment

	(a)		(b)	
Element	wt%	Atomic %	wt%	Atomic %
O	2.20	5.83	23.51	49.18
Fe	64.10	48.54	65.86	39.48
Ni	7.18	6.61	3.37	1.92
Cr	15.05	12.24	3.33	2.15
C	7.18	25.27	2.24	6.23
Mn	0.48	0.37	1.68	1.02
Al	0.02	0.04	0.02	0.03
Os	0.00	0.00	0.00	0.00
Mo	0.30	0.45	0.00	0.00
Si	0.30	0.45	0.00	0.00
Total	100.00	100.00	100.00	100.00

2. Variation of H-ZSM-5 Coating amount and Binding Force

Variation of cumulative H-ZSM-5 loading percentage according to the number of binder coating cycles and the different supports is presented in Fig. 3(a). Loading percentage of H-ZSM-5 was calculated as shown in Eq. (1), where w_1 is the weight of the H-ZSM-5 coated WMCR, and w is the weight of the WMCR. Compared to the non-pretreated WMCR, the H-ZSM-5 loading percentage of the pretreated WMCR was obviously high at the same number of binder coating cycles. According to the increase in the number of binder coating cycles, coating amount of H-ZSM-5 generally increased from 1.43 wt% to 10.92 wt% on the non-pretreated WMCR surface and from 4.31 wt% to 15.29 wt% on the pretreated WMCR surface, respectively. In addition, Fig. 3(b) shows results of ultrasonic test for measurement of binding force between WMCR surface and H-ZSM-5. WMCR coated with H-ZSM-5 was immersed in distilled water at ultrasonic bath with 40 kHz

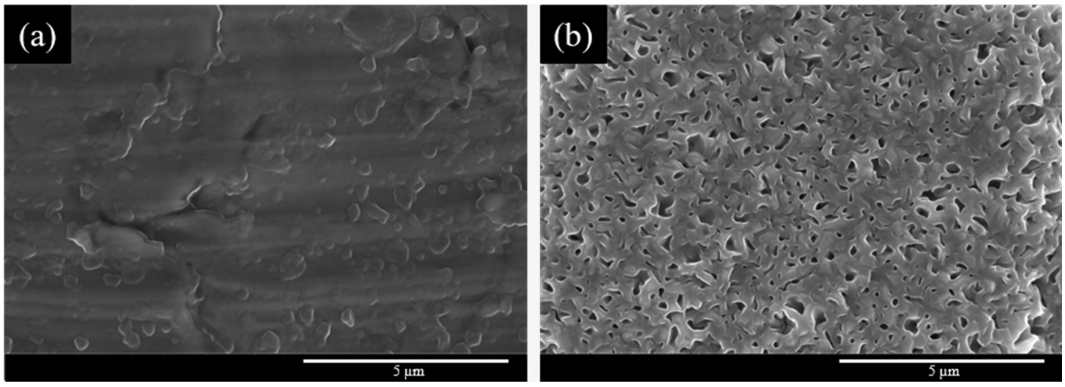


Fig. 2. SEM images of microchannel surface (a) before pretreatment, (b) after pretreatment.

and 300 W for 30 min. Thereafter, treated WMCR was dried at 373 K for 1 h. Weight loss after ultrasonic test was calculated as shown in Eq. (2), where w is the weight of WMCR, w_1 is the weight of WMCR coated with H-ZSM-5, and w_2 is the weight of dried WMCR after ultrasonic test. Depending on increase in the number of binder coating cycles, weight loss decreased from 80.40 wt%

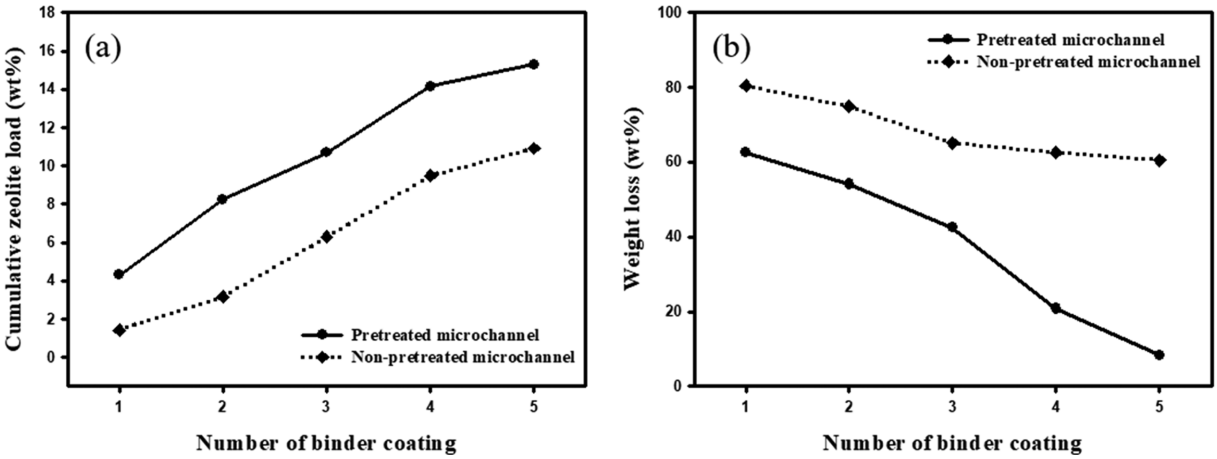


Fig. 3. Results of variation of zeolite loading (a), weight loss of zeolite after ultrasonic test (b) depending on the number of binder coating cycles on the different supports.

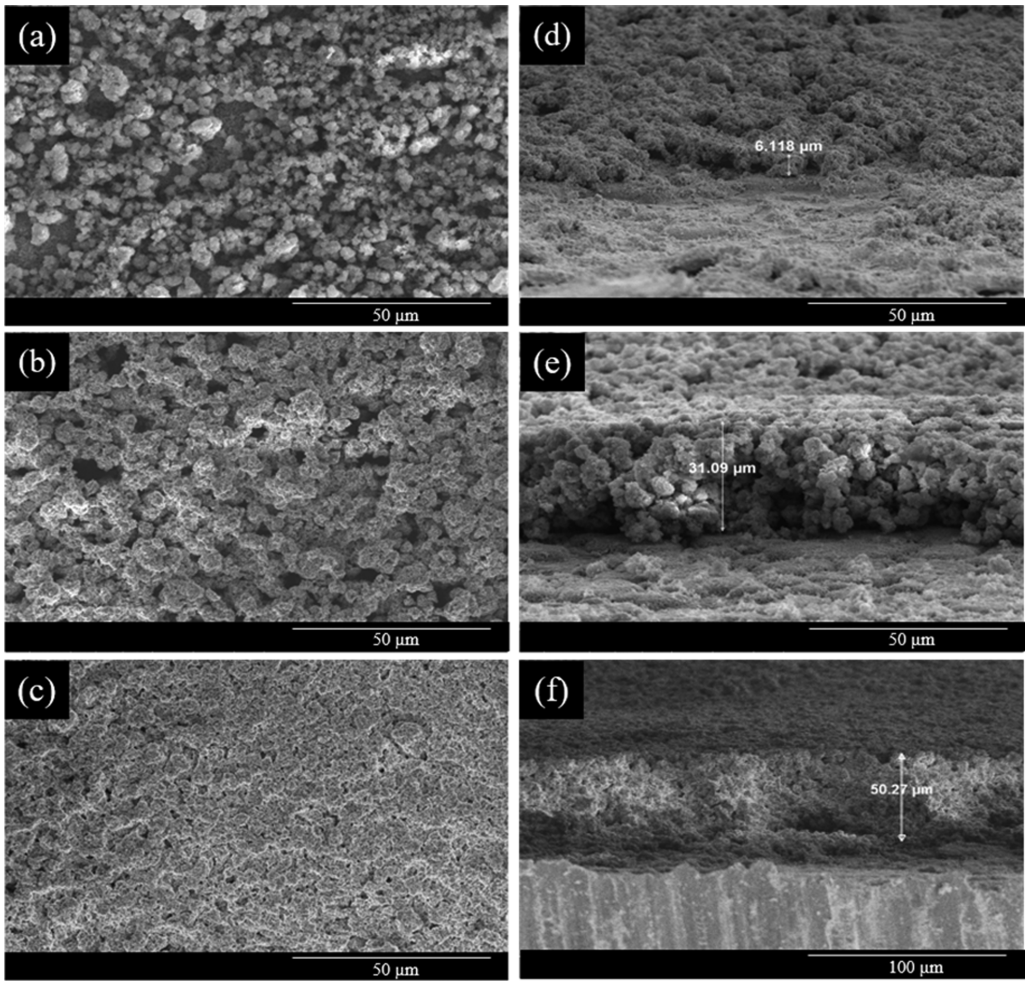


Fig. 4. SEM images of microchannel surface (a) 1-binder coated WMCR, (b) 3-binder coated WMCR, (c) 5-binder coated WMCR, and cross section (d) 1-binder coated WMCR, (e) 3-binder coated WMCR, (f) 5-binder coated WMCR.

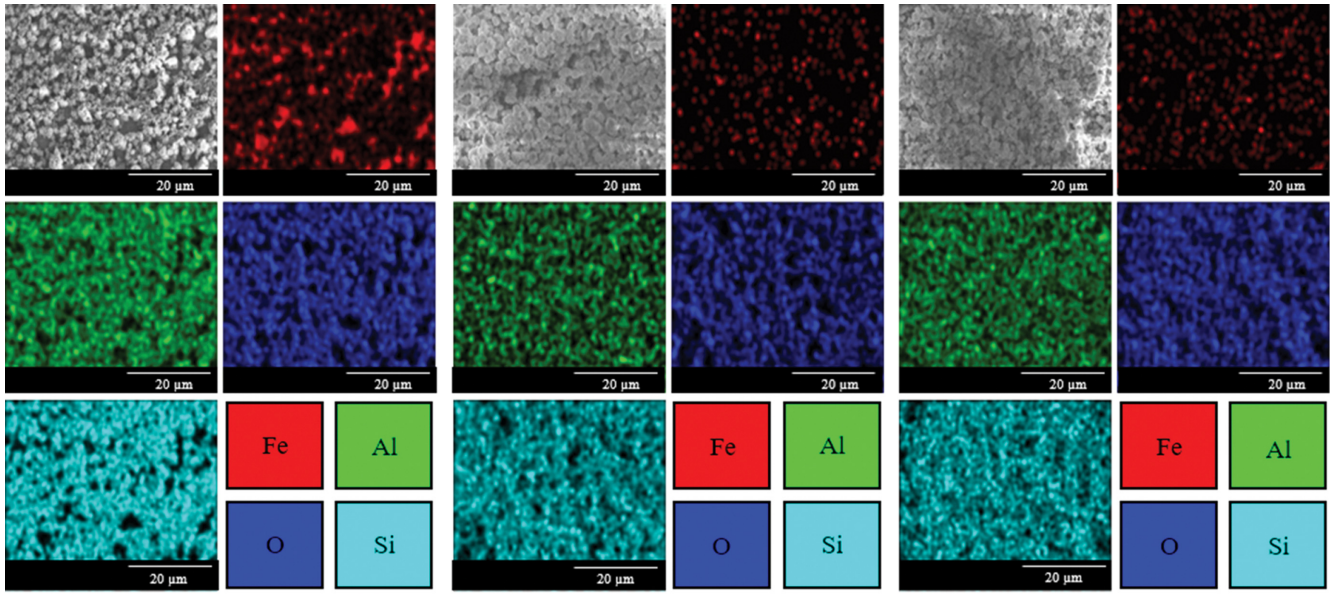


Fig. 5. Results of EDS mapping for the WMCR surface coated with H-ZSM-5 (a) 1-binder coated WMCR (b) 3-binder coated WMCR (c) 5-binder coated WMCR.

to 60.57 wt% on the non-pretreated WMCR, and from 62.50 wt% to 8.28 wt% on the pretreated WMCR. Formation of oxide layer may be attributed to increase in amount of H-ZSM-5 coating and binding force between WMCR surface and H-ZSM-5.

$$\text{Loading percentage (wt\%)} = \frac{w_1 - w}{w} \times 100\ (\%) \quad (1)$$

$$\text{Weight loss (wt\%)} = \frac{w_1 - w_2}{w_1 - w} \times 100\ (\%) \quad (2)$$

3. Characteristics of WMCR Coated with H-ZSM-5

Fig. 4 shows results of SEM image depending on binder coating cycles. Fig. 4(a), (b) and (c) exhibit SEM image of 1-, 3- and 5-binder coated WMCR surface, respectively. H-ZSM-5 on WMCR surface existed densely according to increase in the number of binder coating cycles. In addition, SEM images of cross section about WMCR coated with H-ZSM-5 are presented in Fig. 4(d), (e) and (f). Thickness of H-ZSM-5 coating layer on the WMCR increased from 6.118 μm to 50.27 μm, depending on increase in the number of binder coating cycles. Fig. 5 shows results of EDS-mapping analysis about binder coated WMCRs. As result of EDS-mapping, Fe, the main component of stainless steel, was hidden by Si, Al, O, the main component of H-ZSM-5, according to increase in the number of binder coating cycles.

4. Catalytic Reaction

A heat sink about non-coated, 1-, 3-, and 5-binder coated WMCR is shown in Fig. 6, and the heat sink was calculated, as shown in Eq. (3). In the present study, heat loss naturally occurring in the reactor was calculated to determine heat sink. The heat loss calibration was conducted by comparing between heat loss of blank test and heat loss of N_2 atmosphere test. At blank test, no fluid flowed into the reactor, and at N_2 atmosphere test, flow rate of N_2

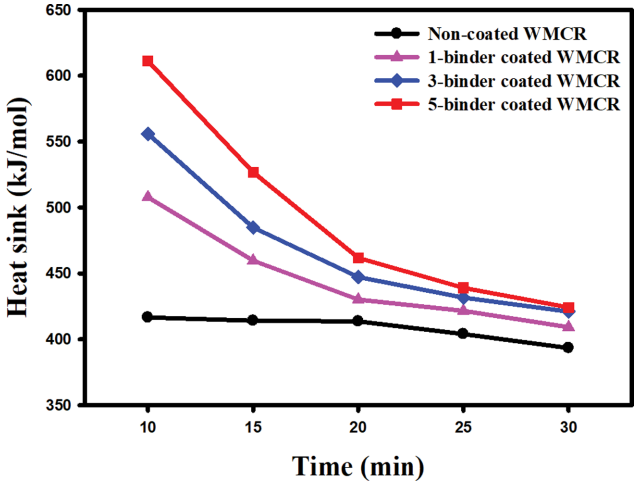


Fig. 6. Variation of heat sink depending on the number of binder coating cycles during catalytic reaction.

was maintained at 0.5 L/min into the reactor. In ideal gas, C_p value of N_2 was 1.13 kJ/kg·K from standard temperature and pressure (STP) condition at 823 K. As a result, calibrated heat loss was determined as 584.95 kJ/mol at 823 K. The calculated heat sink from Eq. (3) was maximum at 10 min, the value decreased in order of 5-binder coated WMCR (611.06 kJ/mol)>3-binder coated WMCR (555.91 kJ/mol)>1-binder coated WMCR (507.76 kJ/mol)>non-coated WMCR (416.59 kJ/mol). Its result may be attributed to increase in coating amount of H-ZSM-5 and improvement of stability of H-ZSM-5 coating layer on WMCR surface. However, the heat sink decreased after 10 min; the result can be considered from stability of H-ZSM-5 coating layer and catalytic deactivation. In the case of 1- and 3-binder coated WMCR, not only cata-

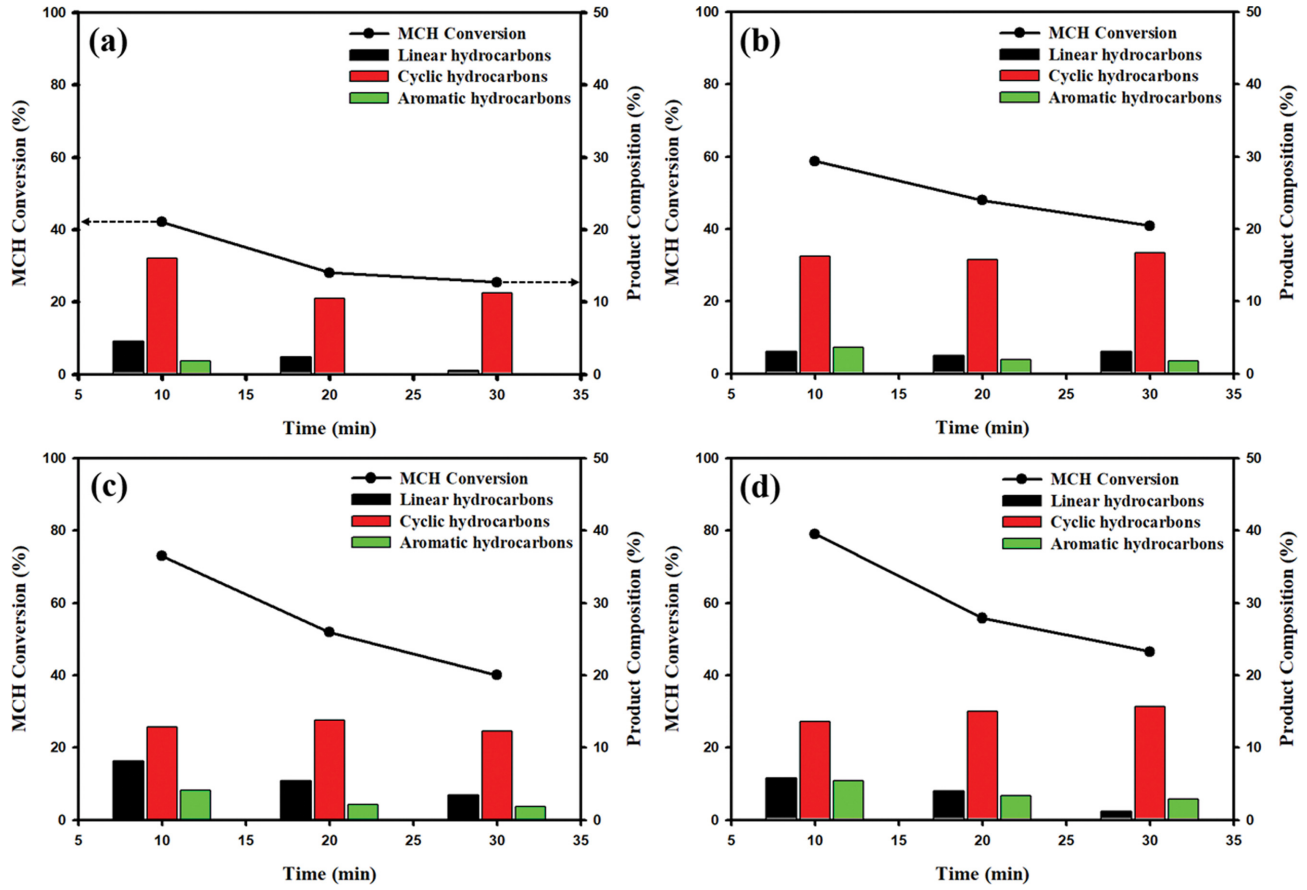


Fig. 7. Hydrocarbon composition of liquid products and MCH conversion during catalytic reaction (a) non-coated WMCR, (b) 1-binder coated WMCR, (c) 3-binder coated WMCR, (d) 5-binder coated WMCR.

lytic deactivation but also instability of H-ZSM-5 coating layer on WMCR surface may be attributed to decrease in heat sink activity. However, in the case of 5-binder coated WMCR with relatively high stability of H-ZSM-5 coating layer, rapid catalytic deactivation of commercial H-ZSM-5 may be predominantly attributed to decrease in heat sink performance. Catalytic deactivation decreased in the following order: 5-binder coated WMCR (30.58%)>3-binder coated WMCR (24.27%)>1-binder coated WMCR (19.41%)> non-coated WMCR (5.89%). Fig. 7 shows results of MCH conversion and composition of liquid products. MCH conversion directly related with heat sink was determined, as shown in Eq. (4). At 10 min, MCH conversion was the highest value for all WMCRs; the values decreased in order of 5-binder coated WMCR (79.02%)>3-binder coated WMCR (72.95%)>1-binder coated WMCR (58.75%)> non-coated WMCR (42.11%). Moreover, MCH conversion decreased from 10 min to 30 min because of catalytic deactivation. The composition of cyclic hydrocarbons about liquid products formed by catalytic reaction was higher than other hydrocarbons. Several studies reported that aromatic hydrocarbons might cause catalytic deactivation because these can behave as coke precursor [41-43]. When reaction time was 10, 20, and 30 min respectively, the of aromatic hydrocarbons increased depending on increase in H-ZSM-5 coating amount on WMCR surface. These results may be attributed to decrease in not only heat sink but also MCH conversion after 10 min.

$$\text{Heat sink} = \text{Electrical heater input power} + \text{Sensible heat of MCH at 673 K} - \text{Heat loss} \quad (3)$$

$$\text{MCH conversion} = \left(\frac{\text{Initial mole of } n_{MCH} - \text{Final mole of } n_{MCH}}{\text{Initial mole of } n_{MCH}}\right) \times 100\ (\%) \quad (4)$$

The gaseous products (such as hydrogen, C_1-C_4 paraffins and olefins) produced after endothermic decomposition reaction of MCH contribute to the improvement of heat sink [5,16]. Gas conversion was calculated from Eq. (5), and the results are shown in Fig. 8. In comparison with non-coated WMCR and binder coated WMCR, gas conversion remarkably increased by H-ZSM-5 coating layer on WMCR and gas conversion was generally improved depending on increase in the number of binder coating cycles. The value at 10 min decreased in order of 5-binder coated WMCR (53.16%)>3-binder coated WMCR (45.12%)>1-binder coated WMCR (35.77%)>non-coated WMCR (19.77%). Likewise, MCH conversion, gas conversion also decreased from 10 min to 30 min owing to coke formation. Distribution about the number of carbons of liquid products after catalytic reaction is presented in Fig. 9. Catalytic deactivation could be caused by formation of high molecular weight hydrocarbons because catalyst surface could be

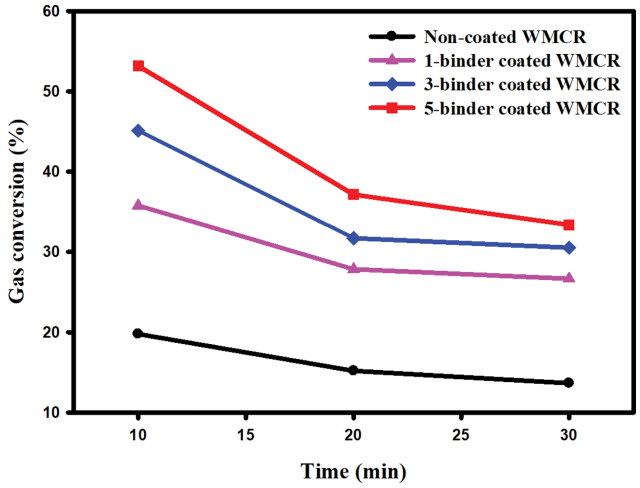


Fig. 8. Gas conversion during catalytic reaction depending on the number of binder coating cycles.

hidden and catalyst pore could be blocked by being forming these products. In addition, because standard enthalpy of formation of these products was lower than standard enthalpy of formation about low molecular weight hydrocarbons, heat absorption may be interrupted by formation of high molecular weight hydrocarbons. Composition of low molecular weight hydrocarbons with less than six carbons increased according to increase in thickness of H-ZSM-5 coating layer on WMCR surface. Its result means that increase in composition of low molecular weight products may be considered to contribute to the improvement of heat sink activity. However, because the composition of high molecular weight hydrocarbons with more than eight carbons simultaneously increased depending on increase in the number of binder coating cycles, catalytic life time may be decreased.

$$\text{Gas conversion} = \left(\frac{\text{Input weight of MCH} - \text{Output weight of liquid product}}{\text{Input weight of MCH}} \right) \times 100\ (\%) \quad (5)$$

5. Coke Analysis

After coke analysis, weight losses about all WMCRs are presented in Fig. 10. Value of weight loss (0.05%) about 5-binder coated WMCR that had the highest catalytic deactivation rate was higher than other WMCRs. These results mean that the composition of aromatic hydrocarbons as coke precursor and high molecular weight hydrocarbons formed on 5-binder coated WMCR were higher

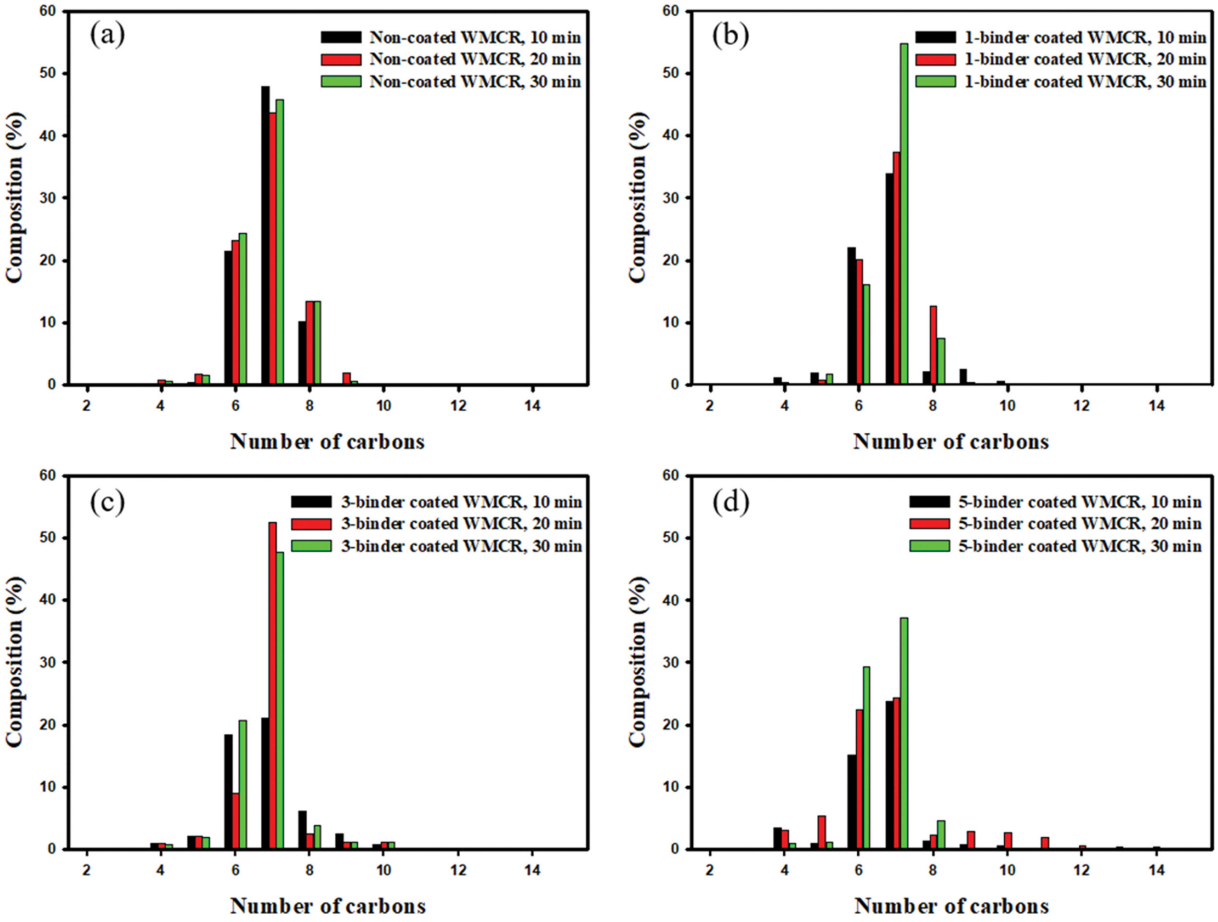


Fig. 9. Distribution of the number of carbons after catalytic reaction at 10, 20, and 30 min (a) non-coated WMCR, (b) 1-binder coated WMCR, (c) 3-binder coated WMCR, (d) 5-binder coated WMCR.

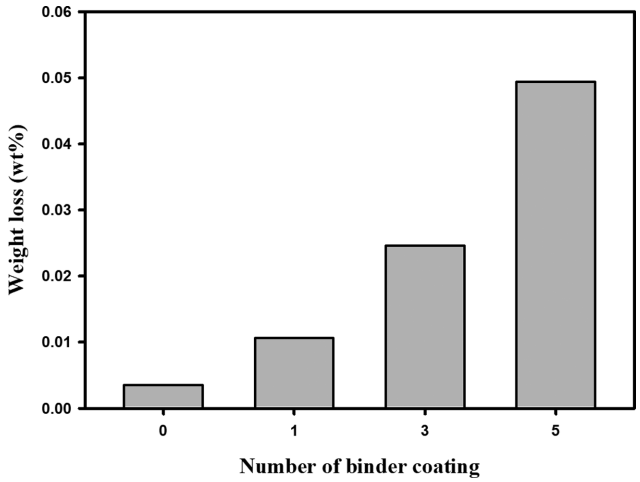


Fig. 10. Weight loss of WMCR depending on the number of binder coating cycles after coke analysis.

than other WMCRs.

CONCLUSIONS

WMCR coated with H-ZSM-5 was successfully prepared by using pretreatment procedure and binder coating method for endothermic decomposition reaction of MCH. H-ZSM-5 loading amount on WMCR surface increased from 10.92 wt% to 15.29 wt% through pretreatment procedure, and not only thickness of H-ZSM-5 coating layer but also stability of coating layer increased from 6.118 μm to 50.27 μm through repetition of binder coating cycle. As the number of binder coating cycles, heat sink performance was generally enhanced during catalytic reaction. As a result, the value of heat sink during catalytic reaction increased from 416.59 kJ/mol to 611.06 kJ/mol. However, when the reaction time exceeded 10 min, catalytic deactivation rate increased from 5.89% to 30.58% because of increase in formation of aromatic hydrocarbons as coke precursor and high molecular weight hydrocarbons. Based on the results, an increase in catalyst loading amount on WMCR surface for catalytic reaction had a trade-off relationship; the increase of catalysts on WMCR had positive effect on overall improvement of heat sink but simultaneously negative effect for catalytic life time. Because catalytic performance and stability of catalyst coating layer on WMCR should be significantly considered, finally, we determined that the best system was 5-binder coated WMCR in endothermic decomposition reaction of MCH using WMCR.

ACKNOWLEDGEMENTS

This research was funded by a Grant-in-aid from the Korean Agency for Defense Development (ADD) funded by the Korean Defense Acquisition Program Administration (DAPA) and the Korean Ministry of National Defense (MND).

REFERENCES

1. M. C. Shin, J. I. Moon, J. H. Jung, B. H. Jeong and J. H. Park, *React. Kinet. Mech. Catal.*, **126**, 761 (2019).
2. N. Gascoin, P. Gillard, E. Dufour and Y. Touré, *J. Thermophys. Heat Transf.*, **21**, 86 (2007).
3. D. T. Wickham, J. R. Engel, S. Rooney and B. D. Hitch, *J. Propul. Power*, **24**, 55 (2008).
4. Y. Guo and R. Lin, *J. Zhejiang Univ.-SCI A*, **6**, 632 (2005).
5. J. Kim, S. H. Park, B. H. Chun, B. H. Jeong, J. S. Han and S. H. Kim, *Catal. Today*, **185**, 47 (2012).
6. T. H. Lee, H. Jeong, B. H. Jeong, J. S. Han, M. Y. Gim, D. H. Kim, S. H. Kim and K. B. Lee, *Appl. Surf. Sci.*, **511**, 145398 (2020).
7. A. C. Nixon and H. T. Henderson, *Ind. Eng. Chem. Prod. Res. Dev.*, **5**, 87 (1966).
8. X. E, Y. Zhang, J.-J. Zou, L. Wang and X. Zhang, *Ind. Eng. Chem. Res.*, **53**, 12312 (2014).
9. D. R. Sobel and L. J. Spadaccini, *J. Eng. Gas. Turbines Power*, **119**, 344 (1997).
10. R. Jiang, G. Liu, X. He, C. Yang, L. Wang, X. Zhang and Z. Mi, *J. Anal. Appl. Pyrolysis*, **92**, 292 (2011).
11. H. Lander and A. C. Nixon, *J. Aircr.*, **8**, 200 (1971).
12. H. Wu and G. Li, *Appl. Catal. A: Gen.*, **423-424**, 108 (2012).
13. K. H. Song, S. K. Jeong, B. H. Jeong, K. Y. Lee and H. J. Kim, *Catalysts*, **10**, 1149 (2020).
14. H. L. Zhao, F. X. Meng, W. Guo, J. J. Zou and X. W. Zhang, *J. Fuel Chem. Technol.*, **36**, 462 (2008).
15. L. Hou, N. Dong and D. Sun, *Fuel*, **103**, 1132 (2013).
16. B. Liu, Q. Zhu, L. X. Qin, X. J. Li, X. Y. Li, S. Y. Tang and J. L. Wang, *J. Propul. Power*, **32**, 801 (2016).
17. S. S. Vasu, D. F. Davidson, Z. Hong and R. K. Hanson, *Energy Fuels*, **23**, 175 (2009).
18. K. Narayanaswamy, H. Pitsch and P. Pepiot, *Combust. Flame*, **162**, 1193 (2015).
19. F. Meng, G. Liu, S. Qu, L. Wang, X. Zhang and Z. Mi, *Ind. Eng. Chem. Res.*, **49**, 8977 (2010).
20. K. H. Song, S. K. Jeong, K. T. Park, K. Y. Lee and H. J. Kim, *Fuel*, **276**, 118010 (2020).
21. G. Liu, J. Guo, F. Meng, X. Zhang and L. Wang, *Chin. J. Chem. Eng.*, **22**, 875 (2014).
22. B. Liu, S. Lu, E. Liu, X. Hu and J. Fan, *Korean J. Chem. Eng.*, **35**, 867 (2018).
23. H. Huang, H. Zhu, Q. Zhang and C. Li, *Korean J. Chem. Eng.*, **36**, 210 (2019).
24. N. Xue, L. Nie, D. Fang, X. Guo, J. Shen, W. Ding and Y. Chen, *Appl. Catal. A Gen.*, **352**, 87 (2009).
25. J. Luo, B. V. Bhaskar, Y. H. Yeh and R. J. Gorte, *Appl. Catal. A: Gen.*, **478**, 228 (2014).
26. T. Blasco, A. Corma and J. Martinez-Triguero, *J. Catal.*, **237**, 267 (2006).
27. H. Sun, B. Shen and J. Liu, *Sep. Purif. Technol.*, **64**, 135 (2008).
28. B. T. Holland, V. Subramani and S. K. Gangwal, *Ind. Eng. Chem. Res.*, **46**, 4486 (2007).
29. R. V. Jasra, B. Tyagi, Y. M. Badheka, V. N. Choudary and T. S. G. Bhat, *Ind. Eng. Chem. Res.*, **42**, 3263 (2003).
30. O. Altin and S. Eser, *Ind. Eng. Chem. Res.*, **40**, 596 (2001).
31. W. Guo, X. Zhang, G. Liu, J. Wang, J. Zhao and Z. Mi, *Ind. Eng. Chem. Res.*, **48**, 8320 (2009).
32. G. Yang, X. Zhang, S. Liu, K. L. Yeung and J. Wang, *J. Phys. Chem.*

Solids, **68**, 26 (2007).
33. L. A. Truter, P. R. Makgwane, B. Zeelie, S. Roberts, W. Böhringer and J. C. Q. Fletcher, *Chem. Eng. J.*, **257**, 148 (2014).
34. P. Avila, M. Montes and E. E. Miró, *Chem. Eng. J.*, **109**, 11 (2005).
35. X. Yao, Y. Zhang, L. Du, J. Liu and J. Yao, *Renew. Sust. Energ. Rev.*, **47**, 519 (2015).
36. P. L. Suryawanshi, S. P. Gumfekar, B. A. Bhanvase, S. H. Sonawane and M. S. Pimplapure, *Chem. Eng. Sci.*, **189**, 431 (2018).
37. G. Kolb and V. Hessel, *Chem. Eng. J.*, **98**, 1 (2004).
38. A. Gavriilidis, P. Angeli, E. Cao, K. K. Yeong and Y. S. S. Wan, *Chem. Eng. Res. Des.*, **80**, 3 (2002).
39. M. K. Kim, S. H. Park, M. C. Shin, C. G. Park, E. Magnone and J. H. Park, *Korean J. Chem. Eng.*, **36**, 1201 (2019).
40. J. M. Zamaro, M. A. Ulla and E. E. Miró, *Catal. Today*, **107-108**, 86 (2005).
41. M. D. Argyle and C. H. Batholomew, *Catalysts*, **5**, 145 (2015).
42. T. H. Lee, M. C. Shin, B. H. Jeong and J. H. Park, *Catal. Today*, **358**, 116 (2020).
43. J. A. Moulijn, A. E van Diepen and F. Kapteijn, *Appl. Catal. A: Gen.*, **212**, 3 (2001).